AIMS Mathematics, 10(10): 22995–23024.
DOI: 10.3934/math.20251022
Received: 14 July 2025
Revised: 08 September 2025
Accepted: 10 September 2025
Published: 10 October 2025

https://www.aimspress.com/journal/Math

Research article

European option valuation under mixed rough Bergomi model equipped with jump factor: a pattern search calibration study

Zhengfang Long[1], **Arezou Karimi**[2] **and Farshid Mehrdoust**[2,*]

[1] Business School, China University of Political Science and Law, Beijing, China
[2] Department of Applied Mathematics, Faculty of Mathematical Sciences, University of Guilan, Rasht, Iran

* **Correspondence:** Email: fmehrdoust@guilan.ac.ir, far.mehrdoust@gmail.com.

Abstract: This paper extends the rough Bergomi model to enhance its accuracy in modeling financial market's dynamics. The proposed model incorporates a jump component into the price process to capture sudden market events. Additionally, the volatility process is enriched by combining two fractional Brownian motions with a common Hurst parameter, which allows for a more precise reflection of short-term volatility dependencies. To ensure arbitrage-free pricing, a risk-neutral probability measure is introduced. Under this measure, the martingale property of the price is verified, and the existence of a solution for the model is established. A combined formula for pricing a European call option is subsequently derived, and a pattern search algorithm is proposed for the model's calibration. The results demonstrate that the proposed model is capable of accurately reproducing market prices across both short- and long-term maturities. Furthermore, the model successfully reproduces the observed volatility smile and skew in the market. This capability affirms the model's effectiveness in capturing and understanding the empirical dynamics of financial markets.

Keywords: rough volatility; fractional Brownian motion; jump process; variance curve
Mathematics Subject Classification: 60G22, 62P05, 90C20

1. Introduction

The Black and Scholes [1] model, despite its foundational role in option pricing theory, relies on several simplifying assumptions, including constant volatility, normally distributed returns, and the absence of transaction costs. These assumptions may not accurately reflect the complexities of real-world financial markets. Empirical evidence suggests that asset price movements often exhibit characteristics such as sudden jumps, time-varying volatility, and long-range dependence, which are not adequately captured by the Black-Scholes framework. To address the limitations of

the Black-Scholes model, researchers have incorporated jump processes into the price dynamics. Merton [2] pioneered this approach by introducing a compound Poisson process to model sudden price jumps, representing unexpected events such as news announcements or economic crises. On the other hand, recognizing the time-varying nature of volatility, researchers have developed stochastic volatility models to capture its dynamic behavior. These models introduce additional sources of randomness to describe fluctuations in volatility, often employing hidden Markov processes or other stochastic processes. In this regard, Bates [3] proposed one of the most influential frameworks by combining stochastic volatility with jump-diffusion dynamics. This so-called Bates model extends the Heston [4] model by incorporating jump components in the asset price, thereby providing a more realistic description of asset returns and implied volatility surfaces. The Bates model has become a cornerstone in option pricing and serves as a benchmark for subsequent developments in the literature. Kou [5] further refined these models by exploring alternative jump distributions, enhancing their ability to capture different types of market events. Building on this line of research, Zaevski et al. [6] replaced the standard Poisson jumps with infinite-activity jumps modeled through tempered stable Lévy processes. There is strong evidence that this choice more accurately captures both the structure of the underlying asset (S&P 500, under the real-world measure) and the option structure (under the risk-neutral measure).

Recent work, such as Tian and Zhang [7], has integrated stochastic volatility, jumps, and transaction costs into a unified framework, providing a more comprehensive approach to option pricing. Li and Wang [8] proposed a model for European option pricing with Lévy-driven interest rates and asset prices, accounting for potential defaults and credit events. Hilliard et al. [9] investigated the impact of different loss and evaluation functions on the accuracy of parameter estimation for jump-diffusion models, highlighting the sensitivity of pricing results to the choice of calibration methodology. He and Lin [10] derived an analytical solution for the price of foreign exchange options under a sophisticated model incorporating stochastic volatility and correlated interest rates, providing a valuable tool for practitioners. Recent studies have explored various advanced applications of differential equations and mathematical analysis in financial modeling. In particular, Mesgarani et al. [11] proposed a fuzzy-based efficiency assessment framework for financial systems, highlighting the importance of incorporating systemic uncertainties in evaluating financial performance. Additionally, Wu et al. [12] investigated portfolio optimization under uncertain financial models, demonstrating how sophisticated mathematical techniques can improve decision-making under uncertainty. Incorporating the insights from these works, our study distinguishes itself by integrating mixed fractional Brownian motion with jump components for European option pricing. This approach not only extends classical stochastic volatility models but also provides a versatile framework that is applicable to a broader range of financial and applied mathematical problems.

While traditional stochastic volatility models have proven effective in capturing certain aspects of volatility dynamics, they may not adequately capture short-term dependencies. Gatheral et al. [13] observed that financial volatility often exhibits short-range dependence, a characteristic captured by fractional Brownian motion (fBm) with a Hurst exponent less than 0.5. To accurately model this behavior, they introduced the rough fractional stochastic volatility (RFSV) model. To simplify the RFSV model, Bayer et al. [14] proposed the rough Bergomi model. By removing the mean-reversion parameter, this model relies solely on a variance curve to determine logarithmic volatility. Empirical studies have shown that the rough Bergomi model generates option prices and volatility patterns that

closely align with real-world observations. Building on this work, Jacquier et al. [15] investigated the dynamics of the volatility index (VIX) index and forward variance curves within the framework of the rough Bergomi model. They developed efficient pricing algorithms for VIX futures and options. The rough Bergomi model has demonstrated superior performance compared with traditional Markovian stochastic volatility models, particularly in reproducing realistic implied volatility smiles for short-term maturities. Meanwhile, El Euch and Rosenbaum [16] delved into the realm of rough Heston models, a class of stochastic volatility models that has gained significant attention in recent years. By incorporating fBm into the volatility process, these models offer a more realistic representation of short-term market dynamics.

To further explore the implications of rough volatility models, Horvath et al. [17] investigated the pricing of volatility derivatives within this framework. These models have gained significant attention due to their ability to capture the complex and short-range dependent nature of financial market volatility. Alòs and León [18] provided a clear and accessible introduction to fractional and rough volatility models, which have gained significant attention in recent years for their ability to capture the complex and short-range dependent nature of financial market dynamics more accurately than traditional models. Ma and Wu [19] addressed a key computational challenge in the application of rough volatility models: the efficiency of simulating sample paths. Despite their ability to accurately capture market dynamics, these models often require computationally intensive simulation techniques. To enhance the flexibility and realism of rough volatility models, Tong and Liu [20] introduced the threshold rough Heston model to price barrier options. By incorporating a threshold mechanism, this model offers a more nuanced approach to modeling volatility dynamics. To further advance the field, Shi et al. [21] focused on developing efficient numerical methods to price options under multivariate rough volatility models. These models are capable of capturing the complex dynamics of financial markets, including correlations between different asset classes and time-varying volatility.

Bianchi et al. [22] examined the roughness of volatility processes by applying the Lamperti transform. This mathematical technique enables more accurate and efficient estimation of the Hurst exponent, a key parameter characterizing the roughness of a time series. The impact of rough stochastic volatility models extends beyond financial markets. Dupret et al. [23] explored the implications of these models for long-term life insurance pricing, where traditional stochastic volatility models often fall short in capturing the complexities of financial market volatility. To further improve volatility forecasting, Zhu et al. [24] focused on incorporating regularity modifications. These modifications adjust the roughness of stochastic processes, such as fBm, to better capture financial market dynamics. Hainaut [25] further extended the analysis by exploring the pricing of spread and exchange options in a market characterized by rough volatility and sudden jumps. Hainaut developed a mathematical framework involving differential equations to calculate the characteristic function of log-returns, a crucial component in option pricing. Karimi et al. [26] examined the pricing and calibration of American call options using the two-factor rough Bergomi model. Their findings indicate that this model accurately captures both historical and future option price dynamics, including the volatility smile. More recently, Karimi and Mehrdoust [27] proposed a semimartingale approximation for the volatility process within the framework of the RFSV model. After a thorough examination of the statistical properties inherent in this novel volatility process, a methodology was introduced for estimating its parameters. This estimation procedure leveraged the VIX index, and the findings demonstrated that the newly developed volatility process accurately reproduces the observed

characteristics of the VIX index.

The classic rough Bergomi model, despite its capability to model volatility, is limited in its ability to account for sudden market shocks or jumps. To address this shortcoming, this paper introduces a novel mixed rough Bergomi model that offers a more accurate representation of market volatility, particularly in the context of unexpected events and short-term dependencies between volatilities. By incorporating a jump component into the price dynamics and combining two fBms with the same Hurst index in the volatility process, the proposed model significantly enhances its ability to capture the intricate dynamics of the market. The key contributions of this paper are as follows. This paper introduces a mixed rough Bergomi model and derives a risk-neutral probability measure for it. The martingale property and the existence of a solution for this model are rigorously examined. A combined formula for the price of a European call option under this model is derived, enabling its practical applications in financial markets. Finally, the model's parameters are calibrated using the pattern search algorithm.

The remainder of this paper is structured as follows. In Section 2, the proposed model and its key characteristics are examined in detail. Section 3 delves into the pricing of European call options under the proposed model. Section 4 introduces the pattern search algorithm, which is employed to calibrate the model parameters. In Section 5, the practical application of the proposed model to real-world market data is discussed. Finally, Section 6 concludes the paper by summarizing the key findings and contributions.

2. Framework of the model

In this section, we introduce the RFSV model, the rough Bergomi model, and our proposed model. We subsequently derive a risk-neutral probability measure for our proposed model. Finally, we discuss the martingale property and the existence of a solution to the proposed model.

Financial market volatility is a significant factor influencing investment decisions. Accurate volatility modeling is crucial for risk assessment, asset pricing, and other financial applications. In recent years, researchers have sought models that can more accurately capture the complex and nonlinear characteristics of volatility. The RFSV model is a novel approach developed to describe the behavior of financial market volatility. This model is based on the findings of Gatheral et al. [13]. They conducted a study on high-frequency volatility data. Their analysis led to the conclusion that volatility exhibits characteristics similar to the fBm with $H \in (0, \frac{1}{2})$. This finding prompted them to introduce the RFSV model with the physical probability measure $\mathbb{P}$ as follows:

$$\begin{aligned} dS_t &= \varpi_t S_t dt + V_t S_t dB_t^{\mathbb{P}}, \\ d\log(V_t) &= \kappa(\mu - \log V_t)dt + \eta dW_t^{H,\mathbb{P}}, \quad t \in [0, T], \end{aligned}$$

where

$$W_t^{H,\mathbb{P}} = \sqrt{2H} \int_0^t (t-s)^{H-\frac{1}{2}} dW_s^{\mathbb{P}},$$

ϖ_t is drift term, B_t is a standard Brownian motion, $\mu \in \mathbb{R}$, and κ and η are positive parameters. B_t and W_t^H are two correlated processes with the correlation coefficient $\rho \in [-1, 1]$.

On the other hand, the forward variance curve, as a crucial tool in forecasting future volatility, has attracted significant attention from market participants. Studying the behavior of volatility under the influence of this curve significantly contributes to a better understanding of market dynamics and risk

management. Hence, Bayer et al. [14] proposed a version of the RFSV model by setting the mean-reversion parameter (κ) to zero. This modification effectively removes the mean-reverting component from the volatility process, allowing it to be driven solely by the forward variance curve. This model (the rough Bergomi model) with the physical probability measure $\mathbb{P}$ is as follows:

$$dS_t = \varpi_t S_t dt + \sqrt{V_t} S_t dB_t^{\mathbb{P}},$$

$$V_t = \mathbb{E}^{\mathbb{P}}[V_t|\mathcal{F}_s]\,\mathcal{E}\left(\eta\sqrt{2H}\int_0^t (t-s)^{H-\frac{1}{2}} dW_s^{\mathbb{P}}\right) = \mathbb{E}^{\mathbb{P}}[V_t|\mathcal{F}_s]\,\mathcal{E}\left(\eta\tilde{W}_t^{\mathbb{P}}\right),$$

where

$$\tilde{W}_t^{\mathbb{P}} = \sqrt{2H}\int_0^t (t-s)^{H-\frac{1}{2}} dW_s^{\mathbb{P}},$$

and $\mathbb{E}^{\mathbb{P}}[V_t|\mathcal{F}_s] = \chi_s(t)$ is the forward variance curve, a deterministic function that describes the market's expectation of future variance at time t, as seen from time s. Specifically, $\mathbb{E}^{\mathbb{P}}[V_t|\mathcal{F}_0] = \chi_0(t)$ is the initial forward variance curve, representing the market's expectation of future variance at the beginning of the time horizon; $\eta > 0$ is the volatility of volatility; $H \in (0, \frac{1}{2})$; and $\mathcal{E}$ is the Dolean-Dade exponential that, for a zero-mean Gaussian random variable $\mathcal{A}$ is as follows:

$$\mathcal{E}(\mathcal{A}) = \exp\left(\mathcal{A}_t - \frac{1}{2}\mathbb{E}\left[|\mathcal{A}_t|^2\right]\right).$$

Theorem 2.1. *Let the volatility be driven by the following stationary Gaussian process:*

$$V_t = \lambda\exp\left(\kappa_1 + \int_0^t \psi(t-u)dW_s\right) + (1-\lambda)\exp\left(\kappa_2 + \int_0^t \phi(t-u)dW_s\right),$$

where $\psi(.)$ and $\phi(.)$ are continuous and well-defined functions. Then, the volatility process can be shown to be a forward variance curve and, importantly, a martingale. For $s < t$, we observe that

$$V_t = \mathbb{E}^{\mathbb{P}}[V_t|\mathcal{F}_s]\left[\lambda\mathcal{E}\left(\int_s^t \psi(t-u)dW_s\right) + (1-\lambda)\mathcal{E}\left(\int_s^t \phi(t-u)dW_s\right)\right],$$

where $\mathcal{E}$ represents the Doléan-Dade exponential and $\lambda \in [0,1]$.

Proof. We have

$$\begin{aligned}
\mathbb{E}^{\mathbb{P}}[V_t|\mathcal{F}_s] &= \mathbb{E}^{\mathbb{P}}\left[\lambda\exp\left(\kappa_1 + \int_0^t \psi(t-u)dW_s\right) + (1-\lambda)\exp\left(\kappa_2 + \int_0^t \phi(t-u)dW_s\right)\middle|\mathcal{F}_s\right] \\
&= \lambda\left[\exp\left(\kappa_1 + \int_0^s \psi(t-u)dW_s\right)\mathbb{E}^{\mathbb{P}}\left[\exp\left(\int_s^t \psi(t-u)dW_s\right)\right]\right] \\
&\quad + (1-\lambda)\left[\exp\left(\kappa_2 + \int_0^s \phi(t-u)dW_s\right)\mathbb{E}^{\mathbb{P}}\left[\exp\left(\int_s^t \phi(t-u)dW_s\right)\right]\right] \\
&= \lambda\left[\exp\left(\left(\kappa_1 + \int_0^s \psi(t-u)dW_s\right) + \frac{1}{2}\mathbb{E}^{\mathbb{P}}\left[\left(\int_s^t \psi(t-u)dW_s\right)^2\right]\right)\right] \\
&\quad + (1-\lambda)\left[\exp\left(\left(\kappa_2 + \int_0^s \phi(t-u)dW_s\right) + \frac{1}{2}\mathbb{E}^{\mathbb{P}}\left[\left(\int_s^t \phi(t-u)dW_s\right)^2\right]\right)\right].
\end{aligned}$$

Since the expected value of the last term is independent of the filtration up to time s, the filtration condition becomes irrelevant. Substituting this into the volatility process formula yields the desired result

$$\begin{aligned} V_t &= \lambda\left[\exp\left(\kappa_1 + \int_0^s \psi(t-u)dW_s + \int_s^t \psi(t-u)dW_s\right)\right] \\ &\quad + (1-\lambda)\left[\exp\left(\kappa_2 + \int_0^s \phi(t-u)dW_s + \int_s^t \phi(t-u)dW_s\right)\right] \\ &= \mathbb{E}^{\mathbb{P}}[V_t|\mathcal{F}_s]\left[\lambda\exp\left(\int_s^t \psi(t-u)dW_s - \frac{1}{2}\mathbb{E}^{\mathbb{P}}\left(\int_s^t \psi(t-u)dW_s\right)^2\right)\right. \\ &\quad \left. + (1-\lambda)\exp\left(\int_s^t \phi(t-u)dW_s - \frac{1}{2}\mathbb{E}^{\mathbb{P}}\left(\int_s^t \phi(t-u)dW_s\right)^2\right)\right], \end{aligned}$$

where $\mathcal{E}(.)$ is the Doléan-Dade exponential. It follows that the last term possesses the martingale property.

Mixed rough Bergomi model equipped with jump factor

On the basis of Theorem 2.1 and the jump process, we can define the following model under physical probability measure $\mathbb{P}$:

$$\begin{aligned} dS_t &= \varpi_t S_t dt + \sqrt{V_t} S_t dB_t^{\mathbb{P}} + S_t(y_t - 1)dN_t^{\mathbb{P}}, \\ V_t &= \mathbb{E}^{\mathbb{P}}[V_t|\mathcal{F}_s]\left[\lambda\mathcal{E}\left(\eta_1\tilde{W}_t^{\mathbb{P}}\right) + (1-\lambda)\mathcal{E}\left(\eta_2\tilde{W}_t^{\mathbb{P}}\right)\right], \end{aligned} \tag{2.1}$$

where $y(t)$ and $N(t)$ are the jump size and Poisson process, respectively; $\mathbb{E}^{\mathbb{P}}[V_t|\mathcal{F}_s] > 0$, $\eta_1, \eta_2 > 0$; and $\tilde{W}_t^{\mathbb{P}}$ is as follows:

$$\tilde{W}_t^{\mathbb{P}} = \sqrt{2\beta+1}\int_0^t (t-s)^{\beta} dW_s^{\mathbb{P}},$$

such that $\beta \in (-\frac{1}{2}, 0)$, and $W_t^{\mathbb{P}}$ and $B_t^{\mathbb{P}}$ are correlated for $\rho \in [-1, 1]$.

In this study, we assume independence between price jumps and the volatility process. This assumption, besides offering analytical tractability, ensures that the price process remains a martingale under the risk-neutral measure (in fact, the martingale property holds whenever the correlation is less than or equal to zero). Nevertheless, in practice, jumps and volatility may exhibit dependence, particularly during periods of market stress. Hence, extending the model to allow for nonzero correlations would be a valuable direction for future research.

Theorem 2.2. *Under the risk-neutral measure $\mathbb{Q}$, the dynamics of the model* (2.1) *are as follows:*

$$\begin{aligned} dS_t &= (r_t - \lambda_J k)S_t dt + \sqrt{V_t} S_t dB_t^{\mathbb{Q}} + S_t(y_t - 1)dN_t^{\mathbb{Q}}, \\ V_t &= \mathbb{E}^{\mathbb{Q}}[V_t|\mathcal{F}_s]\left[\lambda\mathcal{E}(\eta_1\tilde{W}_t^{\mathbb{Q}}) + (1-\lambda)\mathcal{E}(\eta_2\tilde{W}_t^{\mathbb{Q}})\right], \end{aligned} \tag{2.2}$$

where r is the risk-free rate, and $B^{\mathbb{Q}}$ is $\mathbb{Q}$-Brownian motion, and $\tilde{W}_t^{\mathbb{Q}}$ is $\mathbb{Q}$-fBm.

Proof. Let r is the risk-free rate by applying Girsanov's theorem, we have

$$dB_t^{\mathbb{Q}} = dB_t^{\mathbb{P}} + \frac{\varpi_t - r_t}{\sqrt{V_t}}dt. \tag{2.3}$$

To ensure arbitrage-free pricing under the risk-neutral measure, the jump component of the price process must be properly adjusted. The original jump term $(Y_t - 1)dN_t$ contributes a predictable drift that must be neutralized. Therefore, we replace it by its compensated version:

$$(Y_t - 1)dN_t - \mathbb{E}[(Y_t - 1)dN_t]. \tag{2.4}$$

This adjustment ensures that the expected contribution from the jump component is zero under the risk-neutral measure, which is necessary for the discounted price process to be a martingale. Assuming $\mathbb{E}[Y_t - 1] = k$ and $\mathbb{E}[dN_t] = \lambda_J dt$, we have

$$\mathbb{E}[(Y_t - 1)dN_t] = \lambda_J k\, dt. \tag{2.5}$$

Consequently, the risk-neutral dynamics of the price process are

$$dS_t = (r - \lambda_J k)S_t dt + \sqrt{V_t} S_t dB_t^{\mathbb{Q}} + S_t(Y_t - 1)dN_t^{\mathbb{Q}}, \tag{2.6}$$

where r is the risk-free rate. The compensator term $-\lambda_J k$ guarantees that the expected drift is correctly adjusted, so the discounted price remains a martingale, satisfying the no-arbitrage condition.

Now, we obtain the volatility process in the model (2.1) under the risk-neutral measure. Since $W_t^{\mathbb{P}}$ and $B_t^{\mathbb{P}}$ are correlated, we have

$$W_t^{\mathbb{P}} = \rho dB_t^{\mathbb{P}} + \sqrt{1-\rho^2}\, \overset{*}{dB}_t^{\mathbb{P}},$$

where the Brownian motions $B_t^{\mathbb{P}}$ and $\overset{*}{B}_t^{\mathbb{P}}$ are independent. Now, we define

$$\overset{*}{dB}_t^{\mathbb{Q}} = \overset{*}{dB}_t^{\mathbb{P}} + \upsilon_t dt,$$

where υ is the market price of risk. Now, we have

$$\begin{aligned} W_t^{\mathbb{P}} =& \rho dB_t^{\mathbb{P}} + \sqrt{1-\rho^2}\, \overset{*}{dB}_t^{\mathbb{P}} \\ =& \rho dB_t^{\mathbb{Q}} + \sqrt{1-\rho^2}\, \overset{*}{dB}_t^{\mathbb{Q}} + \left(-\rho \frac{\varpi_t}{\sqrt{V_t}} - \sqrt{1-\rho^2}(\upsilon_t)\right) dt \\ =& W_t^{\mathbb{Q}} + \left(-\rho \frac{\varpi_t}{\sqrt{V_t}} - \sqrt{1-\rho^2}(\upsilon_t)\right) dt, \end{aligned}$$

which can be rewritten as follows:

$$W_t^{\mathbb{P}} = W_t^{\mathbb{Q}} + \Gamma_t dt.$$

Define

$$K_\beta(s,t) = \left[\lambda\eta_1 + (1-\lambda)\eta_2\right] \sqrt{2\beta+1}(t-s)^\beta. \tag{2.7}$$

In particular, $\mathbb{E}^{\mathbb{P}}[V_t | F_s]$ is adapted to the filtration produced by $W^{\mathbb{P}}$ and $W^{\mathbb{Q}}$. Then, the logarithm of the volatility process is as follows:

$$V_t = \mathbb{E}^{\mathbb{P}}[V_t | \mathcal{F}_s] \exp\left\{ \int_t^u K_\beta(s,t) dW_s^{\mathbb{P}} - \lambda \frac{\eta_1^2}{2}(t-u)^{2\beta+1} - (1-\lambda)\frac{\eta_2^2}{2}(t-u)^{2\beta+1} \right\}$$

$$= \mathbb{E}^{\mathbb{P}}\left[V_t \,|\mathcal{F}_s\right]\left\{\int_t^u K_\beta(s,t)\left(dW_s^{\mathbb{Q}} + \Gamma_s ds\right) - \lambda\frac{\eta_1^2}{2}(t-u)^{2\beta+1} \; -(1-\lambda)\frac{\eta_2^2}{2}(t-u)^{2\beta+1}\right\}$$

$$= \mathbb{E}^{\mathbb{P}}\left[V_t \,|\mathcal{F}_s\right]\left[\lambda\mathcal{E}\left(\eta_1\tilde{W}_t^{\mathbb{Q}}\right) + (1-\lambda)\mathcal{E}\left(\eta_2\tilde{W}_t^{\mathbb{Q}}\right)\right] \times \exp\left\{\int_t^u K_\beta(s,t)\Gamma_s ds\right\}.$$

We put

$$\mathbb{E}^{\mathbb{Q}}\left[V_t \,|\mathcal{F}_s\right] = \mathbb{E}^{\mathbb{P}}\left[V_t \,|\mathcal{F}_s\right] \times \exp\left\{\int_t^u K_\beta(s,t)\Gamma_s ds\right\}.$$

As a result,

$$V_t = \mathbb{E}^{\mathbb{Q}}\left[V_t \,|\mathcal{F}_s\right]\left[\lambda\mathcal{E}(\eta_1\tilde{W}_t^{\mathbb{Q}}) + (1-\lambda)\mathcal{E}(\eta_2\tilde{W}_t^{\mathbb{Q}})\right],$$

where

$$\tilde{W}_t^{\mathbb{Q}} = \sqrt{2\beta+1}\int_0^t (t-s)^\beta dW_s^{\mathbb{Q}}.$$

In the subsequent, we will examine the martingale property within the context of the proposed model under the risk-neutral measure. The martingale property stipulates that the conditional expectation of the underlying asset's future price, given the current information set, is equal to its present value. This property serves as a cornerstone for fair option valuation. Indeed, if the underlying asset price process deviates from the martingale property, arbitrage opportunities may emerge, leading to distorted option prices. For instance, if the price of a specific stock exhibits a deterministic upward trend, an investor could exploit this predictability by purchasing the stock and simultaneously selling a put option on it, thereby generating riskless profits. Such strategies, predicated on anticipating market trends, are precluded in a risk-neutral framework.

Definition 2.1. *A stochastic process $(X_t)_{t\geq 0}$ adapted to a filtration $(\mathcal{F}_t)_{t\geq 0}$ is called a* true martingale *if*

(1) X_t is $\mathcal{F}_t$-measurable for all $t \geq 0$,
(2) $\mathbb{E}[|X_t|] < \infty$ for all $t \geq 0$, and
(3) $\mathbb{E}[X_t \mid \mathcal{F}_s] = X_s$ for all $0 \leq s \leq t$.

Theorem 2.3. *Suppose $Y_t := \int_0^t K_\beta(s,t)dW_s^{\mathbb{Q}}$ defines a Gaussian process, where $K_\beta(s,t) = [\lambda\eta_1 + (1-\lambda)\eta_2]\sqrt{2\beta+1}(t-s)^\beta$, and $V : [0,\infty)\times\mathbb{R} \to \mathbb{R}^+$ is bounded on $[0,T]\times(-\infty,a]$, for each $T, a > 0$. Then, $e^{-rt}S_t$ $t \geq 0$ defined by the model* (2.2) *is a true martingale under the risk-neutral measure $\mathbb{Q}$, if $\rho \leq 0$.*

Proof. We closely follow Gassiat [28] with some modifications. Since $e^{-rt}S_t$ is a supermartingale, it will be a martingale on $[0,T]$ if and only if $\mathbb{E}^{\mathbb{Q}}[e^{-rT}S_T] = S_0$. Let $\iota_n := \inf\left\{t \geq 0, \int_0^t K_\beta(s,t)dW_s^{\mathbb{Q}} = n\right\}$, then since V_t is bounded on $[0,T]\times(-\infty,n]$, we define

$$T \wedge \iota_n = \min\{T, \iota_n\}. \tag{2.8}$$

Additionally, since V_t is bounded, then $\mathbb{E}\left[e^{-r(T\wedge\iota_n)}S_{T\wedge\iota_n}\right] < \infty$, and hence we have

$$S_0 = \mathbb{E}\left[e^{-r(T\wedge\iota_n)}S_{T\wedge\iota_n}\right].$$

According to Eq (2.8), we obtain

$$S_0 = \mathbb{E}^{\mathbb{Q}}[e^{-r(T\wedge\iota_n)}S_{T\wedge\iota_n}] = \mathbb{E}^{\mathbb{Q}}[e^{-rT}S_T 1_{\{T<\iota_n\}}] + \mathbb{E}^{\mathbb{Q}}[e^{-r\iota_n}S_{\iota_n}1_{\{T\geq\iota_n\}}].$$

The stopping time ι_n emphasizes that $\mathbb{E}^{\mathbb{Q}}[e^{-rT}S_T 1_{\{T<\iota_n\}}]$ converges to $\mathbb{E}[e^{-rT}S_T]$ as n tends to infinity, and then we have

$$S_0 - \mathbb{E}^{\mathbb{Q}}\left[e^{-rT}S_T\right] = \lim_{n\uparrow\infty} \mathbb{E}^{\mathbb{Q}}\left[e^{-r\iota_n}S_{\iota_n}1_{\{T\geq\iota_n\}}\right],$$

we define

$$e^{-r\iota_n}S_{\iota_n}1_{\{T\geq\iota_n\}} = \begin{cases} S_0, & if \;\; T \geq \iota_n, \\ 0, & otherwise. \end{cases}$$

We then have $\mathbb{E}^{\mathbb{Q}}[e^{-r\iota_n}S_{\iota_n}1_{\{T\geq\iota_n\}}] = S_0\tilde{\mathbb{P}}_n(T \geq \iota_n)$, such that

$$\tilde{W}_t^n = W_t^{\mathbb{Q}} - \rho\int_0^{t\wedge\iota_n} V(s, Y_s)ds$$

is a Brownian motion under $\tilde{\mathbb{P}}_n$. For $t \leq \iota_n$, we have

$$Y_t = \int_0^t K_\beta(s,t)\left(d\tilde{W}_s^n + \rho V(s,Y_s)ds\right) = \tilde{Y}_t + \rho\int_0^t K_\beta(s,t)V(s,Y_s)ds,$$

where $\tilde{W}_s^n$ is a Brownian motion under $\tilde{\mathbb{P}}_n$, and

$$\tilde{Y}_t = \int_0^t K_\beta(s,t)d\tilde{W}_s^n.$$

If $\rho \leq 0$, then $Y_t \leq \tilde{Y}_t$, and we obtain

$$\lim_{n\uparrow\infty}\tilde{\mathbb{P}}_n(\iota_n \leq T) \leq \lim_{n\uparrow\infty}\tilde{\mathbb{P}}(\tilde{\iota}_n \leq T) = \lim_{n\uparrow\infty}\mathbb{P}(\sup_{t\in[0,T]} Y_t \geq n) = 0,$$

where

$$\tilde{\iota}_n := \inf\{t \geq 0, \int_0^t K_\beta(s,t)d\tilde{W}_s^n = \mathrm{n}\};$$

hence, $e^{-rt}S_t$ is a true martingale.

Remark 2.1. *Although the market is incomplete due to rough volatility and jumps, the model can still be used for derivative pricing. By working under the canonical risk-neutral measure $\mathbb{Q}$, the discounted price process is a martingale, and the option prices are computed as the $\mathbb{Q}$-expected discounted payoff. This provides a well-defined and tractable pricing framework even in the presence of incompleteness.*

Assumption 2.1. *Given a probability space $(\Omega, \mathcal{F}, \mathbb{Q})$ and a σ-finite measure space $(D, \mathcal{D}, m)$, we consider a $\mathbb{R}^d$-valued Brownian motion $(W_t)_{t\geq 0}$ $(d \in \mathbb{N})$ and a Poisson random measure $N(dtdy)$ on $\mathbb{R}^+ \times D$ with the intensity measure $\lambda_{J(0,\infty)} \otimes m$ and let $\tilde{N} := N - \lambda_{J(0,\infty)} \otimes m$. Moreover, we consider the following condition:*
(1) (Local Lipschitz condition) For any integer $n \geq 1$ a positive constant $\mathcal{K}_n$ exists such that, for any $t \in [0,T]$ and any $S, \xi, r \in \mathbb{R}^d$ with $|S| \vee |\xi| \vee |r| \leq n$, we have

$$\begin{aligned} &\left|f(t,S,\xi,r) - f(t,\bar{S},\bar{\xi},\bar{r})\right|^2 + \left|g(t,S,\xi,r) - g(t,\bar{S},\bar{\xi},\bar{r})\right|^2 + \int\left|z(t,S,\xi,r) - z(t,\bar{S},\bar{\xi},\bar{r})\right|^2 m(dy) \\ \leq &\mathcal{K}_n\left(\left|S-\bar{S}\right|^2 + \left|\xi-\bar{\xi}\right|^2 + |r-\bar{r}|^2\right). \end{aligned}$$

Theorem 2.4. *Assuming that Assumption 2.1 holds, there is a unique solution $S(t)$ to the equation*

$$dS_t = f(t, S_t, \xi_t, r_t)dt + g(t, S_t, \xi_t, r_t)dW_t^{\mathbb{Q}} + \int z_{t^-}(t, S_t, \xi_t, r_t, y)\tilde{N}^{\mathbb{Q}}(dtdy). \tag{2.9}$$

See Appendix A1 for the detailed proof.

3. Option pricing

In this section, we derive a combined formula for the price of a European option under the proposed model, utilizing the Hull and White [29] approach.

Definition 3.1. *The European call option price with a maturity T and a strike price K is given by*

$$C(S, 0) = e^{-rT}\mathbb{E}^{\mathbb{Q}}\left[\max\left(S_T - K, 0\right)\right].$$

Theorem 3.1. *Suppose that the stock process and volatility process are uncorrelated ($\rho = 0$) in the model* (2.2)*. Then, the European call option under the model* (2.2) *is as follows:*

$$C(S(0), K, T, r_{n,T}, \sigma_{n,T}) = \mathbb{E}^{\mathbb{Q}}\left[\sum_{n=0}^{\infty} e^{-\lambda_J T}\frac{(\lambda_J T)^n}{n!}\left(S(0)\mathcal{N}(d_{1,n}) - e^{-rT}K\mathcal{N}(d_{2,n})\right)\right], \tag{3.1}$$

where

$$\begin{aligned} d_{1,n} &= \frac{1}{\sigma_{n,T}\sqrt{T}}\left[\log\frac{S(0)}{K} + (r_{n,T} - \frac{1}{2}\sigma_{n,T}^2)T\right], \\ d_{1,n} &= d_{1,n} + \sigma_{n,T}\sqrt{T}, \end{aligned}$$

and

$$r_{n,T} = r - \lambda_J k - \frac{1}{2}\bar{V} + \frac{n\mu_J}{T} + \frac{1}{2}\sigma_{n,T}^2, \quad \sigma_{n,T} = \sqrt{\bar{V} + \frac{n\sigma_J^2}{T}}.$$

Proof. As established by Theorem 2.2, we have

$$dS(t) = (r - \lambda_J k)S(t)dt + \sqrt{V(t)}S(t)dW^{\mathbb{Q}}(t) + (y(t) - 1)S(t)dN^{\mathbb{Q}}(t). \tag{3.2}$$

As guaranteed by Theorem 2.4, the aforementioned differential equation possesses a unique solution. Hence, to determine the solution to Eq (3.2), we invoke Itô's formula:

$$\begin{aligned} df(S(t), t) = &\frac{\partial f(S(t), t)}{\partial t}dt + b_t\frac{\partial f(S(t), t)}{\partial x}dt + \frac{\sigma^2}{2}\frac{\partial^2 f(S(t), t)}{\partial x^2}dt + \sigma_t\frac{\partial f(S(t), t)}{\partial x}dW(t) \\ &+ \left[f(S(t^-) + \Delta S(t)) - f(S(t^-))\right]. \end{aligned}$$

Thus we get

$$d\ln S(t) = \frac{\partial \ln S(t)}{\partial t}dt + (r - \lambda_J k)S(t)\frac{\partial \ln S(t)}{\partial S(t)}dt + \frac{\bar{V}S^2(t)}{2}\frac{\partial^2 \ln S(t)}{\partial S^2(t)}dt$$

$$
\begin{aligned}
&+ \sqrt{\bar{V}} S(t) \frac{\partial \ln S(t)}{\partial S(t)} dW^{\mathbb{Q}}(t) + [\ln y(t) S(t) - \ln S(t)] \\
&= (r - \lambda_J k) S(t) \frac{1}{S(t)} dt + \frac{\bar{V} S^2(t)}{2} \left(-\frac{1}{S^2(t)} \right) dt + \sqrt{\bar{V}} S(t) \frac{1}{S(t)} dW^{\mathbb{Q}}(t) \\
&+ [\ln y(t) + \ln S(t) - \ln S(t)] \\
&= (r - \lambda_J k)\, dt - \frac{\bar{V}}{2} dt + \sqrt{\bar{V}} dW^{\mathbb{Q}}(t) + \ln y(t),
\end{aligned}
$$

where $\bar{V} = \int_0^t V(s) ds$. Integrating the process above over the interval from 0 to t gives

$$
\ln S(t) = \ln S(0) + \left(r - \frac{\bar{V}}{2} - \lambda_J k \right) t + \sqrt{\bar{V}} W^{\mathbb{Q}}(t) + \sum_{m=1}^{N(t)} \ln y_m.
$$

Since $\ln y_m \sim \mathcal{N}(\mu_J, \sigma_J^2)$, $\sum_{m=1}^{N(t)} \ln y_m \sim \mathcal{N}(n\mu_J, n\sigma_J^2)$. On the other hand, we have $\sqrt{\bar{V}} W^{\mathbb{Q}}(t) \sim \mathcal{N}(0, \bar{V}t)$. Due to the independence of the Brownian movement paths and jump sizes, we have

$$
\begin{aligned}
\sqrt{\bar{V}(t)} W^{\mathbb{Q}}(t) + \sum_{m=1}^{N(t)} \ln y_m &\sim \mathcal{N}(0 + n\mu_J, \bar{V}t + n\sigma_J^2) \sim \mathcal{N}(n\mu_J, (\bar{V} + \frac{n\sigma_J^2}{t})t) \\
&\sim n\mu_J + \sqrt{\bar{V} + \frac{n\sigma_J^2}{t}} \sqrt{t} Z,
\end{aligned}
$$

where Z is the standard normal variable. Since $W^{\mathbb{Q}}(t) \sim \sqrt{dt} Z$, then

$$
\sqrt{\bar{V}(t)} W^{\mathbb{Q}}(t) + \sum_{m=1}^{N(t)} \ln y_m \sim n\mu_J + \sqrt{\bar{V} + \frac{n\sigma_J^2}{t}} W^{\mathbb{Q}}(t).
$$

Hence

$$
\begin{aligned}
\ln S(t) - \ln S(0) &= \left(r - \lambda_J k - \frac{1}{2}\bar{V} \right) t + n\mu_J + \sqrt{\bar{V} + \frac{n\sigma_J^2}{t}} W^{\mathbb{Q}}(t) \\
&= \left(r - \lambda_J k - \frac{1}{2}\bar{V} + \frac{n\mu_J}{t} \right) t + \sqrt{\bar{V} + \frac{n\sigma_J^2}{t}} W^{\mathbb{Q}}(t). \qquad (3.3)
\end{aligned}
$$

We can rewrite Eq (3.3) as follows:

$$
\ln S(t) - \ln S(0) = (r_{n,t} - \frac{1}{2}\sigma_{n,t}^2)t + \sigma_{n,t} W^{\mathbb{Q}}(t),
$$

where

$$
r_{n,t} = r - \lambda_J k - \frac{1}{2}\bar{V} + \frac{n\mu_J}{t} + \frac{1}{2}\sigma_{n,t}^2,
$$

and

$$
\sigma_{n,t} = \sqrt{\bar{V} + \frac{n\sigma_J^2}{t}}.
$$

Then

$$S(T) = S(0)\exp\left((r_{n,T} - \frac{1}{2}\sigma_{n,T}^2)T + \sigma_{n,T}W^{\mathbb{Q}}(T)\right), \tag{3.4}$$

where

$$d_{1,n} = \frac{1}{\sigma_{n,T}\sqrt{T}}\left[\log\frac{S(0)}{K} + (r_{n,T} - \frac{1}{2}\sigma_{n,T}^2)T\right],$$
$$d_{1,n} = d_{1,n} + \sigma_{n,T}\sqrt{T}.$$

Equation (3.4) is obtained according to condition $N(t) = n$. $N(t)$ is a Poisson process, then we have

$$\mathbb{P}(N(t) = n) = \frac{(\lambda_J T)^n}{n!}e^{-\lambda_J T}.$$

Hence, the call option value under the proposed model is as follows:

$$\begin{aligned}
&F(S(0), K, T, r_{n,T}, \sigma_{n,T})\\
&= e^{-rT}\mathbb{E}^{\mathbb{Q}}[\max(S(T) - K, 0)]\\
&= \sum_{n=0}^{\infty} e^{-rT}\mathbb{E}^{\mathbb{Q}}[\max(S(T) - K, 0)]\mathbb{P}(N(t) = n)\\
&= \sum_{n=0}^{\infty} e^{-rT}\frac{(\lambda_J T)^n}{n!}\mathbb{E}^{\mathbb{Q}}[\max(S(T) - K, 0)]\\
&= \sum_{n=0}^{\infty} e^{-\lambda_J T}\frac{(\lambda_J T)^n}{n!}e^{-rT}\mathbb{E}^{\mathbb{Q}}[\max(S(T) - K, 0)]\\
&= \sum_{n=0}^{\infty} e^{-\lambda_J T}\frac{(\lambda_J T)^n}{n!}e^{-rT} \times \mathbb{E}^{\mathbb{Q}}\left[\max\left(S(0)\exp\left\{(r_{n,T} - \frac{1}{2}\sigma_{n,T}^2)T + \sigma_{n,T}W^{\mathbb{Q}}(T)\right\} - K, 0\right)\right].
\end{aligned}$$

The Black-Scholes formula gives

$$F(S(0), K, T, r_{n,T}, \sigma_{n,T}) = \sum_{n=0}^{\infty} e^{-\lambda_J T}\frac{(\lambda_J T)^n}{n!}\left(S(0)\mathcal{N}(d_{1,n}) - e^{-rT}K\mathcal{N}(d_{2,n})\right),$$

where

$$d_{1,n} = \frac{1}{\sigma_{n,T}\sqrt{T}}\left[\log\frac{S(0)}{K} + (r_{n,T} - \frac{1}{2}\sigma_{n,T}^2)T\right],$$
$$d_{1,n} = d_{1,n} + \sigma_{n,T}\sqrt{T}.$$

Since $\bar{V} = \int_0^t V(s)ds$, then according to Hull and White [29], we obtain

$$C(S(0), K, T, r_{n,T}, \sigma_{n,T}) = \mathbb{E}^{\mathbb{Q}}\left[\sum_{n=0}^{\infty} e^{-\lambda_J T}\frac{(\lambda_J T)^n}{n!}\left(S(0)\mathcal{N}(d_{1,n}) - e^{-rT}K\mathcal{N}(d_{2,n})\right)\right].$$

4. Calibration

Calibration of a financial model entails adjusting its parameters to align its predictions with the observed market prices, primarily those of the derivatives. This process is often formulated as a least squares problem, seeking to minimize the discrepancy between market prices and model-generated prices. It can be expressed mathematically as follows:

$$\min_{\theta \in \mathrm{X}} f(\theta), \qquad \mathrm{X} \subseteq \mathbb{R}^n,$$

where $f(\theta)$ is the root mean square error (RMSE) function, given by

$$RMSE(\theta) = \sqrt{\frac{1}{u}\sum_{k=1}^{u} \left(\mathcal{P}_k^{Market} - \mathcal{P}_k^{Model}(\theta)\right)^2},$$

where θ is the vector of model's parameters, u is the number of strike prices, $\mathcal{P}_k^{Market}$ is the market price for the strike k, $\mathcal{P}_k^{Model}(\theta)$ is the prices generated by the model for the strike k using the parameter θ, and X is the feasible region for the parameters.

Let $n \in \mathbb{N}$ be fixed and let us consider the equidistant time partition $t_i = i\Delta t$, $i = 0, 1, 2, ..., n$ of $[0, T]$ with $T > 0$ and $\Delta t = \frac{T}{n}$. Furthermore, suppose that m is the number of Monte Carlo simulations such that $j = 1, ..., m$. To compute $\mathcal{P}_k^{\text{Model}}$, Monte Carlo simulation is used in the following clear steps.

(1) **Simulate volatility paths:** Generate m independent sample paths of the stochastic volatility process V_t, including both mixed fractional Brownian motion and jump components:

$$V_{t_i}^j = \lambda \exp\left(\eta_1 W_{t_i}^{H,j} - \frac{1}{2}\eta_1^2 t_i^{2H}\right) + (1-\lambda)\exp\left(\eta_2 W_{t_i}^{H,j} - \frac{1}{2}\eta_2^2 t_i^{2H}\right), \quad i = 0, \ldots, n.$$

(2) **Compute integrated variance:** For each path, calculate the time-integrated variance using trapezoidal numerical integration:

$$V_i^j = \sum_{i=0}^{n-1} \frac{V_{t_i}^j + V_{t_{i+1}}^j}{2}(t_i - t_{i-1}).$$

(3) **Compute option payoff:** For each path, compute the European call option payoff ϕ_k^j for each strike K_k, incorporating the jump-adjusted pricing formula:

$$\varphi_k^j = \sum \exp(-\lambda_J T)\frac{(\lambda_J T)^n}{n!}\left(S(0)\mathcal{N}(a_n) - e^{-rT}K_k\mathcal{N}(b_n)\right),$$

with

$$a_n = \frac{1}{\sqrt{V_i^j + \frac{n\sigma_J^2}{T}T}}\left[\log\frac{S(0)}{K} + \left(r - \lambda_J k - \frac{1}{2}V_i^j + \frac{n\mu_J}{T}\right)T\right],$$

and

$$b_n = a_n + \sqrt{V_i^j + \frac{n\sigma_J^2}{T}T}.$$

(4) **Average across paths:** Compute the Monte Carlo estimate of the model price:

$$\mathcal{P}_k^{Model} = \frac{1}{m}\sum_{j=1}^{m}\varphi_k^j.$$

A pseudo-code version of this procedure is also provided in Appendix A2.

Pattern search algorithm

Direct search requires a set of potential solutions, represented by points P, and a way to compare their quality. A "better" solution, P_1, is denoted as $P_1 \subset P_2$. Ideally, there is a single optimal solution, P^*, that is superior to all other solutions. The basic direct search process begins by selecting a starting point, B_0. A second point, P_1, is then chosen and compared with B_0. If P_1 is better than B_0, it becomes the new base point, B_1; otherwise, B_0 remains the base point. This process continues, with each new point compared with the current base point. Consider the problem of minimizing a function $f(x_1, x_2, ..., x_n)$. A solution point P_i is a vector $(x_{1i}, x_{2i}, ..., x_{ni})$ and we say solution P_i is better than P_j if and only if $f(x_{1i}, x_{2i}, ..., x_{ni}) < f(x_{1j}, x_{2j}, ..., x_{nj})$. The base point, B_r, is the point with the smallest function value among $B_0, P_1, P_2, ..., P_r$. The next trial point, $P_{(r+1)}$, is determined by the current state, Z_r. A trial is considered a success if $P_{(r+1)}$ improves the function value.

A pattern search is a direct search algorithm employed to determine the minimum of a multi-variable function, denoted as $\mathcal{S}(q)$, where $q = \{q_1, q_2, ..., q_K\}$. The algorithm iteratively adjusts the values of q until it converges upon the lowest achievable value of $\mathcal{S}(q)$. This process involves traversing a K-dimensional space through a series of iterative movements. A movement is classified as successful if it results in a reduction in the function value. As previously mentioned, this algorithm iteratively explores a search space to locate a point where a function achievable its minimum value. The search involves two types of movements: exploratory and pattern-based. In exploratory movements, the algorithm seeks local improvements along each coordinate axis. Pattern-based movements, on the other hand, leverage information gathered from exploratory movements to take larger steps towards an optimal solution. This process continues until the algorithm converges to a local optimum or another termination condition is met. Due to its simplicity and the absence of the need for derivative calculations, this algorithm finds extensive applications in various optimization problems (see [30] for more information).

Pattern search algorithms offer an efficient approach to calibrating financial models, particularly when the relationships between the model's parameters and market data are complex and nonlinear. These algorithms initiate by defining an objective function that quantifies the discrepancy between the model's output and real-world data. Subsequently, they iteratively adjust the model's parameters to discover the optimal combination that minimizes this discrepancy. The algorithm employs two types of movements: Exploratory moves that systematically alter each parameter and pattern-based moves that leverage successful past patterns to induce larger, more rapid changes. Through iterative refinement, the algorithm progressively adjusts the model's parameters to achieve the best possible fit with the market data. Due to their flexibility and capacity to handle intricate relationships, these methods constitute a powerful tool for calibrating complex financial models.

A generalized pattern search given an initial guess at a solution x_0 and an initial choice of a step length parameter $\Delta_0 > 0$ is given in Algorithm 1.

Algorithm 1. Generalized pattern search steps

Given $x_0 \in R^n$, $f(x_0)$, $P_0 \in R^{n*p}$, and $\Delta_0 > 0$, for $k = 0, 1, ...$ until convergence, do
1. Find a step s_k using exploratory moves (Δ_k, P_k).
2. If $f(x_k + s_k) < f(x_k)$, then $x_{k+1} = x_k + s_k$.
Otherwise, $x_{k+1} = x_k$.
3. Update (Δ_k, P_k).

Remark 4.1. *In the deterministic setting, the sequence of trial points can be simplified to comparing the candidate point P with the current base point B. If P improves the objective function, B is updated; otherwise, the algorithm stops. While this guarantees convergence to a local optimum, it does not ensure that the global minimum is reached. In our implementation, we maintain the full sequence structure to allow for extensions with multiple starting points and stochastic variations. Sensitivity analyses show that the resulting solution is robust, providing reliable calibration of the model's parameters.*

5. Empirical study

This study conducts a statistical analysis of the SPDR S&P 500 ETF Trust (SPY) stock returns and evaluates the pricing of European call options on this stock. The analysis utilizes daily data for SPY spanning from August 7, 2019, to August 7, 2020. Additionally, European call option prices with maturities of 2, 12, 30, and 72 days are examined. While this period provides sufficient observations for model calibration, it may not capture all market regimes, such as high-volatility periods or financial crises. Future studies could therefore extend the dataset to assess the robustness of the model under a wider range of market conditions.

The initial asset price (S_0) is taken as the closing price of SPY on August 7, 2019 ($S_0 = 287.97$). We use the raw closing price rather than the dividend-adjusted close, as option markets are quoted and settled with respect to the unadjusted underlying price. In this empirical study, we utilize SPY options instead of SPX options due to their exceptional liquidity, high trading volume, and the availability of a richer dataset across a broader range of strikes and maturities. Moreover, their smaller contract size and wider investor base make them particularly suitable for calibration purposes while still effectively capturing the dynamics of the S&P 500 index.

As Figures 1(a) and 1(b) demonstrate, the distribution of SPY stock returns exhibits a significant departure from a normal distribution. This deviation is particularly evident in the distribution's kurtosis and skewness. If the data followed a normal distribution, all data points would align with the theoretical normal distribution curve. However, as shown in Figure 1(b), the data points, especially in the distribution's left and right tails, deviate substantially from this curve. This indicates the presence of rare events with extremely high or low returns occurring more frequently than predicted by a normal distribution. This phenomenon, known as a price jump, signifies sudden shifts in investor's expectations and heightened market volatility. Price jumps can be attributed to unexpected events such as financial crises, changes in monetary policy, or the release of significant news. The presence of jumps in the time series of returns underscores the importance of accurate modeling and considering tail risks in financial analysis. As depicted in Figure 1(c), the autocorrelation plot

reveals a significant positive autocorrelation among successive SPY stock returns. The autocorrelation coefficients for short lags are significantly greater than zero, indicating volatility clustering. In other words, periods of high or low volatility tend to persist. This phenomenon could be attributed to factors such as investor herding, market trends, or the gradual dissemination of new information. The presence of a strong autocorrelation structure in the initial 40 days of the period highlights a unique characteristic of this time frame. This could be due to specific market events, changes in monetary policy, or shifts in investor sentiment during this period. Statistical analyses unequivocally demonstrate that the assumption of a normal distribution for financial market returns is inadequate and cannot fully capture the complex behavior of these markets. Phenomena such as sudden price jumps and volatility clustering, as inherent characteristics of financial markets, necessitate the employment of more sophisticated models. A profound understanding of these phenomena is crucial for investors, risk managers, and financial researchers, as financial models capable of accommodating these features provide powerful tools for accurate market analysis and informed investment decisions.

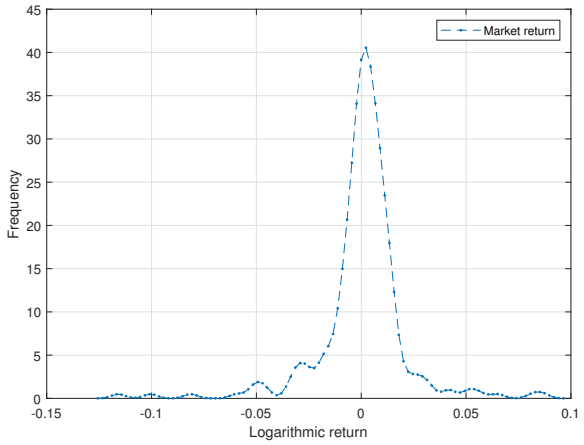

(a) Distribution of returns

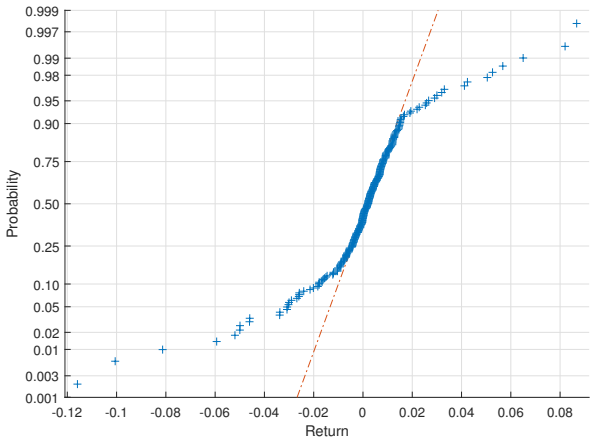

(b) Normality test

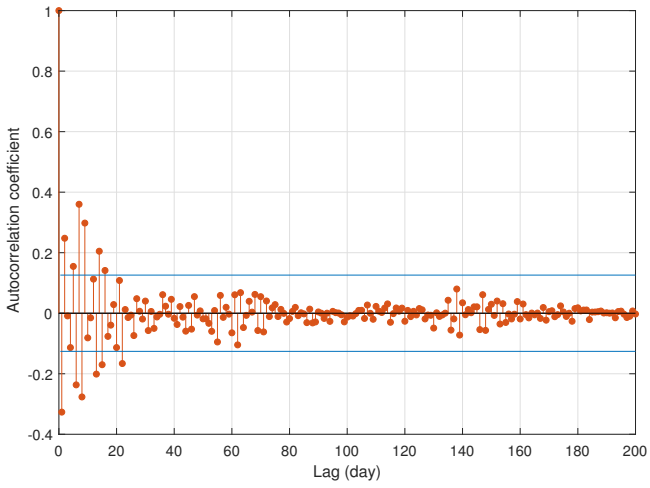

(c) Autocorrelation test

Figure 1. Statistical analyses.

Pursuant to Theorem 3.1, under the assumption of $\rho = 0$, the proposed model successfully generates the implied volatility smiles. Figure 2 empirically validates the model's ability to replicate this distinctive market pattern across various maturity levels. As observed, the implied volatility smile becomes increasingly asymmetric and its level diminishes as the time to maturity increases. This behavior aligns with real-world market observations, where volatility typically decreases with increasing time to maturity. Consequently, the proposed model exhibits a strong capacity to reproduce this crucial characteristic of financial markets.

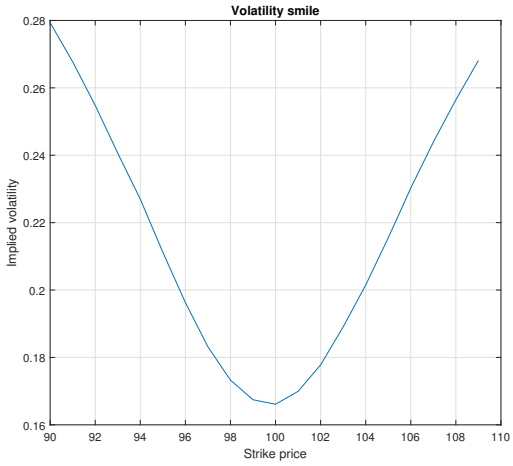

(a) T=0.039

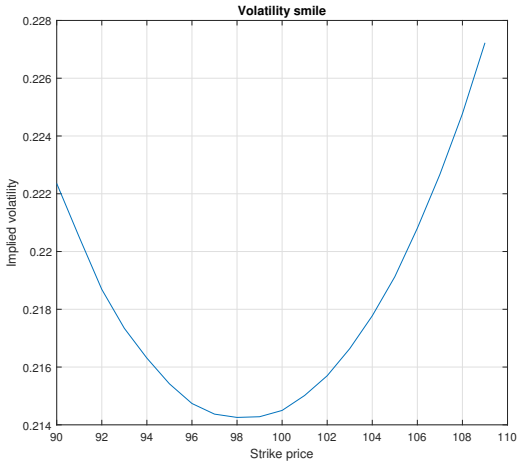

(b) T=0.158

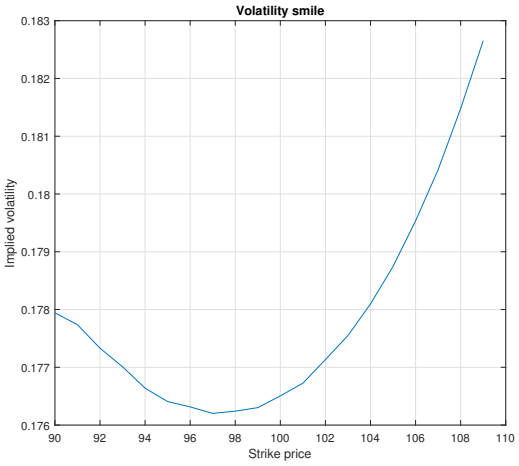

(c) T=0.396

Figure 2. Implied volatility smile under the proposed model. $S_0 = 100, \rho = 0, q = 0.01, r = 0.05, \xi = 0.04, \beta = -0.2, \eta_1 = 1.3, \eta_2 = 0.5, \lambda = 0.1, \lambda_J = 1.5, \mu_J = 0.1, \sigma_J = 0.2$.

A pattern search algorithm was utilized to optimize the parameters of the proposed model and rough Bergomi model and geometric Brownian motion (GBM) model for maturity 12 ($T = 12$). The calibrated parameters are then applied to compute option prices for other maturities. This strategy simplifies the calibration process while preserving the main features of the market option prices across

different maturities. We employ MATLAB's built-in pattern search algorithm to calibrate the model's parameters. The default algorithm settings are summarized in Table 1. The initial parameter values were carefully chosen on the basis of historical estimates and prior studies. Convergence is determined according to MATLAB's default settings: The algorithm stops when the change in the objective function falls below 10^{-6} (FunctionTolerance) or when the maximum number of iterations (200 times the number of parameters) is reached. StepTolerance and MeshTolerance are also set to their default values of 10^{-6}. These default settings are summarized in Table 1.

Table 1. Default settings of MATLAB's pattern search algorithm.

Parameter	**Default value**	**Description**
MaxIterations	$200 \times n$	Maximum number of iterations
MaxFunctionEvaluations	$1000 \times n$	Maximum number of function evaluations
FunctionTolerance (TolFun)	1×10^{-6}	Tolerance of the change in the objective function
StepTolerance (TolX)	1×10^{-6}	Tolerance of the change in the parameters
MeshTolerance	1×10^{-6}	Minimum mesh size for local search
Display	'final'	Level of algorithm output displayed
PollMethod	'GPSPositiveBasis2N'	Method for exploring search directions
MeshExpansionFactor	2	Factor to expand the mesh size
MeshContractionFactor	0.5	Factor to contract the mesh size

The initial values, together with the lower and upper bounds of each model parameter, are reported in Tables 2–4. The calibration parameters are summarized in Tables 5–7. As evidenced by the results in Tables 5–7, the pattern search algorithm used for the calibration of the Black-Scholes, rough Bergomi, and the proposed model, only optimized the interest rate parameter while keeping all other core parameters constant. This behavior is a clear indication of the algorithm getting trapped in a local optimum, a common yet critical challenge in the calibration of complex financial models. The root of this issue can be attributed to two main factors: the non-convex nature of the objective function and the varying sensitivities of the model parameters. The objective function employed for calibrating financial models, commonly defined as the mean squared error between model-generated option prices and observed market prices, is inherently highly non-linear and nonconvex. Such functions often feature flat regions and multiple local minima within the parameter space. Local optimization algorithms, like a pattern search, which do not rely on gradient information and operate by evaluating the objective function in the immediate neighborhood of the current point, are highly susceptible to getting stuck in these local minima. This behavior is particularly pronounced when the initial guess is already located near a local optimum, and subsequent improvements in the objective function fall below the algorithm's tolerance threshold. The parameters of the models do not have a uniform impact on the model's output. The interest rate parameter, for instance, has a very high sensitivity, especially for pricing long-term options. Small changes in this parameter lead to significant changes in the option values. Consequently, the optimization algorithm quickly adjusts the interest rate to minimize the overall error. In contrast, the core parameters of the rough Bergomi and the proposed model (such as the Hurst parameter ($\beta = H - \frac{1}{2}$) and the volatility of volatility (η) have more intricate and non-linear effects. This disparity in sensitivity causes the algorithm to favor the most sensitive parameter, neglecting a thorough exploration of the multi-dimensional space for the less sensitive ones.

Table 2. Parameter settings for the mixed one-factor rough Bergomi model equipped with a jump factor.

	r	q	χ_0	ρ	β	η_1	η_2	λ	λ_J	σ_J
Initial	0.05	0.01	0.01	0	-0.4	1.9	0.5	0.1	1.5	0.2
Lower bound	0.01	0.001	0.01	-0.4	-0.4	1.2	0.3	0.1	0.1	0.1
Upper bound	0.09	0.05	0.05	-0.1	-0.1	1.9	0.9	0.9	2.5	0.8

Table 3. Parameter settings for the rough Bergomi model.

	r	χ_0	β	ρ	η
Initial	0.05	0.02	-0.1	-0.9	0.8
Lower bound	0.01	0.02	-0.49	-0.95	0.8
Upper bound	0.09	0.09	-0.1	-0.1	1.1

Table 4. Parameter settings for the GBM model.

	r	σ
Initial	0.05	0.3
Lower bound	0.01	0.2
Upper bound	0.06	0.8

Table 5. Calibrated parameters of the mixed one-factor rough Bergomi model equipped with a jump factor. We note that $q = \lambda_J k$.

r	q	χ_0	β	η_1	η_2	λ	λ_J	μ_J	σ_J
0.05	0.0178	0.04	-0.2000	1.3000	0.5000	0.1000	0.2000	0.1000	0.2000

Table 6. Calibrated parameters of the rough Bergomi model.

r	χ_0	β	ρ	η
0.05	0.02	-0.1	-0.275	0.8

Table 7. Calibrated parameters of the GBM model.

r	σ
0.01	0.3

To assess the robustness of the calibration procedure for the proposed model, we conducted a sensitivity analysis in two ways.

(1) Sensitivity to the starting point: The algorithm was run using three different sets of initial parameter values.
(2) Sensitivity to maximum run time: The effect of increasing the maximum number of iterations on the calibrated parameters was evaluated.

The results are presented in Tables 8 and 9, showing that only the risk-free rate is adjusted by the algorithm, while other parameters remain stable. Extending the search time does not change the results, indicating that the calibration effectively identifies a local optimum, with sensitivity primarily to the interest rate.

Table 8. Sensitivity analysis of calibrated parameters for the proposed model with respect to different initial guesses.

Parameter	Initial Set 1	Calibrated Set 1	Initial Set 2	Calibrated Set 2	Initial Set 3	Calibrated Set 3
r	0.0110	0.0110	0.0120	0.0198	0.0130	0.0208
q	0.0510	0.0510	0.0520	0.0520	0.0530	0.0530
χ_0	0.0410	0.0410	0.0420	0.0420	0.0430	0.0430
β	-0.3900	-0.3900	-0.3800	-0.3800	-0.3700	-0.3700
η_1	1.3200	1.3200	1.3300	1.3300	1.3400	1.3400
η_2	0.5100	0.5100	0.5200	0.5200	0.5300	0.5300
λ	0.1100	0.1100	0.1200	0.1200	0.1300	0.1300
λ_J	0.2100	0.2100	0.2200	0.2200	0.2300	0.2300
σ_J	0.1100	0.1100	0.1200	0.1200	0.1300	0.1300
μ_J	0.2100	0.4600	0.2200	0.2200	0.2300	0.2300

Table 9. Sensitivity analysis of calibrated parameters for the proposed model with respect to different maxtime in the iterations.

Seconds	r	q	χ_0	β	η_1	η_2	λ	λ_J	μ_J	σ_J
0.5	0.0100	0.0500	0.0400	-0.2000	1.3000	0.5000	0.1000	0.2000	0.1000	0.4500
0.75	0.0100	0.0500	0.0400	-0.2000	1.3000	0.5000	0.1000	0.2000	0.1000	0.4500
0.9	0.0178	0.0500	0.0400	-0.2000	1.3000	0.5000	0.1000	0.2000	0.1000	0.2000

In order to validate the proposed framework, we also examine its special cases. Specifically, when $\lambda = 0$, the model reduces to the classical rough Bergomi model with jumps. To illustrate this, we provide Table 10, which compares the option prices generated by the proposed model with those obtained from the rough Bergomi specification. The results indicate that the two sets of prices are very close to each other, with the proposed model producing slightly higher values due to the positive average jump size. This finding confirms the internal consistency of the model while highlighting the contribution of the additional jump component. Moreover, the results are aligned with standard economic intuition: As the strike price increases, the value of the European call option decreases, whereas an increase in the underlying asset price leads to higher option values. These observations provide further evidence supporting the validity and robustness of the proposed framework.

Table 10. Comparison of the prices of the proposed model and rough Bergomi model when $\lambda = 0$.

S	10	15	20	30
K=9	1.2009 1.2246	6.0258 5.9337	10.9755 10.8700	20.8748 20.6449
K=10	0.5556 0.4812	5.0460 4.9533	9.9951 9.8896	19.8944 19.6645
K=11	0.2036 0.1227	4.0693 3.9732	9.0147 8.9093	18.9141 18.6841
K=12	0.0616 0.0230	3.1081 2.9957	8.0344 7.9289	17.9337 17.7038

The calibration and options pricing results unequivocally demonstrate the superior performance of the proposed model in comparison with the Black-Scholes (GBM model) and rough Bergomi models. As is evident from the pricing of European call options across various maturities (Figures 3–6 and Table 11), the developed model, calibrated using 12 days of data, has accurately reproduced the market prices for both short-term and long-term maturities. This exceptional performance is attributed to the model's ability to capture and accurately model complex market phenomena, including the volatility memory effect and jumps, which are absent in simpler models. In stark contrast, the Black-Scholes model only achieved acceptable pricing accuracy for the $T = 2$ maturity. Its performance for all other maturities was inadequate, primarily due to its inherent assumption of constant volatility. This fundamental limitation prevents the Black-Scholes model from correctly capturing and reproducing market-observed structures such as the volatility smile. Furthermore, the developed model outperformed the rough Bergomi model, indicating that the inclusion of a mixed variance curve and other advanced features allows for a more comprehensive and accurate absorption of complex market dynamics. These findings underscore the critical importance of employing sophisticated models to precisely replicate market behavior.

In the other words, the Black-Scholes model is built on the simplifying assumptions of constant volatility and normally distributed returns. Although these assumptions provide analytical tractability, they are inconsistent with empirical evidence from financial markets. In reality, asset volatility is highly time-varying, return distributions exhibit heavy tails, and asset prices are subject to sudden jumps. Consequently, the Black-Scholes framework fails to reproduce key market phenomena such as implied volatility smiles and skews, which limits its effectiveness for pricing both short- and long-maturity options. The rough Bergomi model improves upon these limitations by incorporating fractional Brownian motion with a Hurst exponent less than 0.5, capturing short-range dependence and the rough behavior of volatility. This allows the model to produce realistic implied volatility smiles, particularly for short maturities, and represents a significant advancement over the Black-Scholes framework. Building on this, the proposed model further enhances the flexibility and realism of volatility modeling by introducing both a jump component and two distinct volatility-of-volatility parameters, η_1 and η_2. The jump process captures sudden, unexpected market shocks, while the dual volatility-of-volatility components allow the model to reflect both short-term fluctuations and long-term persistence in volatility simultaneously. Additionally, the use of two fractional Brownian

motions with a common Hurst exponent H ensures that both short-range and long-range dependencies are accurately reproduced. As a result, the proposed framework not only retains the advantages of the rough Bergomi model but also achieves superior alignment with observed market prices across different maturities. In short-maturity horizons, it effectively replicates the implied volatility smiles and sudden price jumps, whereas in long-maturity horizons, it maintains stability and consistency with the market data. Compared with the Black-Scholes model, which cannot account for these complex dynamics, both the rough Bergomi and the proposed model provide significantly more accurate and flexible option pricing.

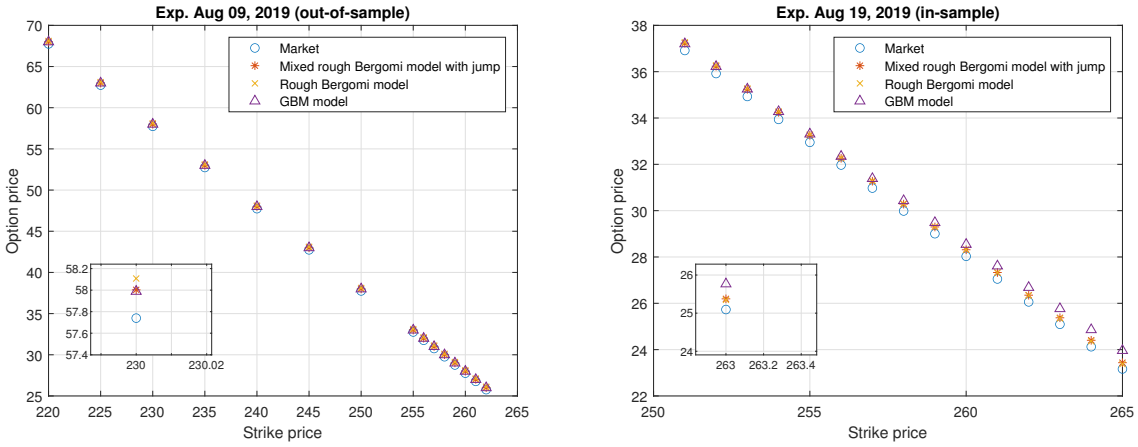

(a) T=2 **(b)** T=12

Figure 3. Comparing European call option prices for T=2 and 12.

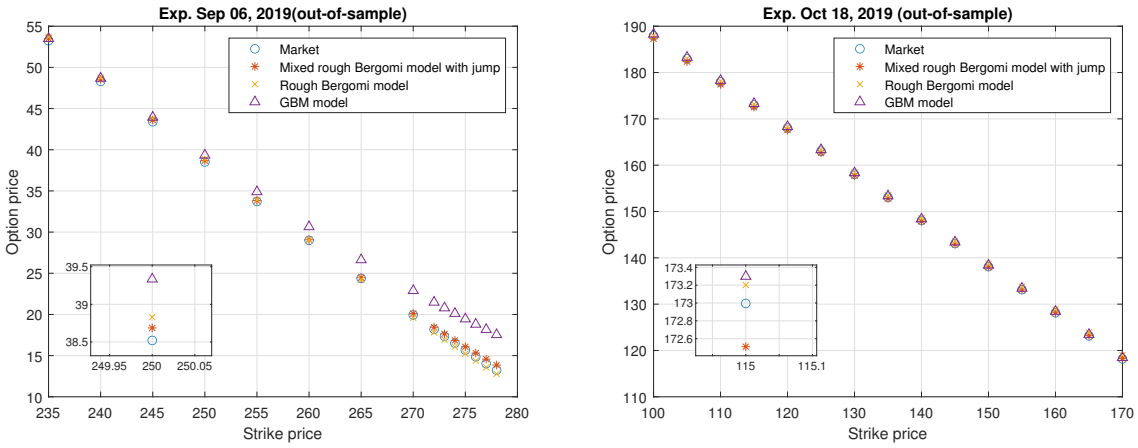

(a) T=30 **(b)** T=72

Figure 4. Comparing European call option prices for T=30 and 72.

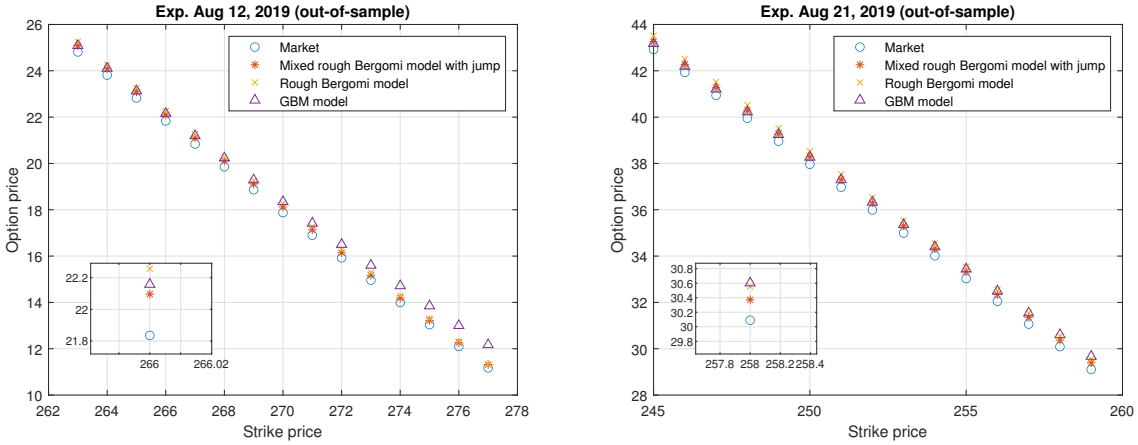

(a) T=5 **(b)** T=14

Figure 5. Comparing European call option prices for T=5 and 14.

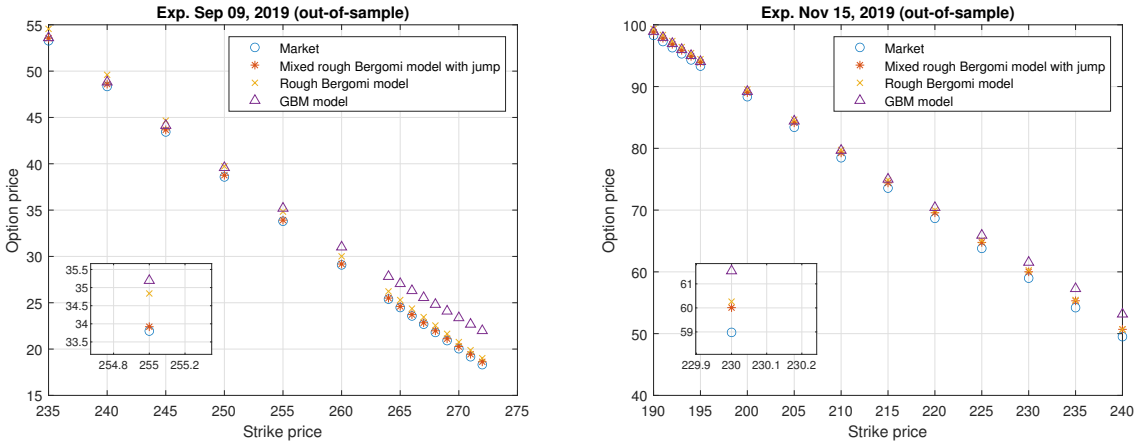

(a) T=33 **(b)** T=100

Figure 6. Comparing European call option prices for T=33 and 100.

Table 11. The MSE for T=12 and out-of-sample data.

Maturity	Mixed rough Bergomi model with jump	Rough Bergomi model	GBM model
T=2	0.2535	0.348	0.229
T=12	0.295	0.317	0.509
T=30	0.327	0.380	2.586
T=72	0.356	0.513	0.592
T=5	0.231	0.357	0.583
T=14	0.320	0.523	0.574
T=33	0.203	0.899	2.334
T=100	0.811	1.161	1.782

The visual results presented in Figures 7 and 8 confirm the proposed model's remarkable ability to accurately reproduce the market's implied volatility surface. These images show a strong alignment between the model's implied volatility and the market's observed volatility across all analyzed maturities, from short-term to long-term. This alignment is particularly evident in the successful reproduction of non-linear structures such as the volatility smile and volatility skew. These structures are characterized by implied volatility being higher for out-of-the-money or in-the-money options compared with at-the-money options. This ability sets the proposed model apart from the limitations of classical models like the Black-Scholes model. The Black-Scholes model, with its assumption of constant volatility, cannot reproduce such market-observed structures. In contrast, our model, by incorporating advanced dynamics such as stochastic volatility, can accurately capture and reproduce these crucial market features. This finding unequivocally demonstrates that the developed model not only reproduces market prices correctly but is also capable of accurately modeling the dynamic implied volatility structure. This capability makes our model a powerful and reliable tool for accurate options pricing, risk management, and analyses of market dynamics, confirming its superiority over classical and even some advanced models.

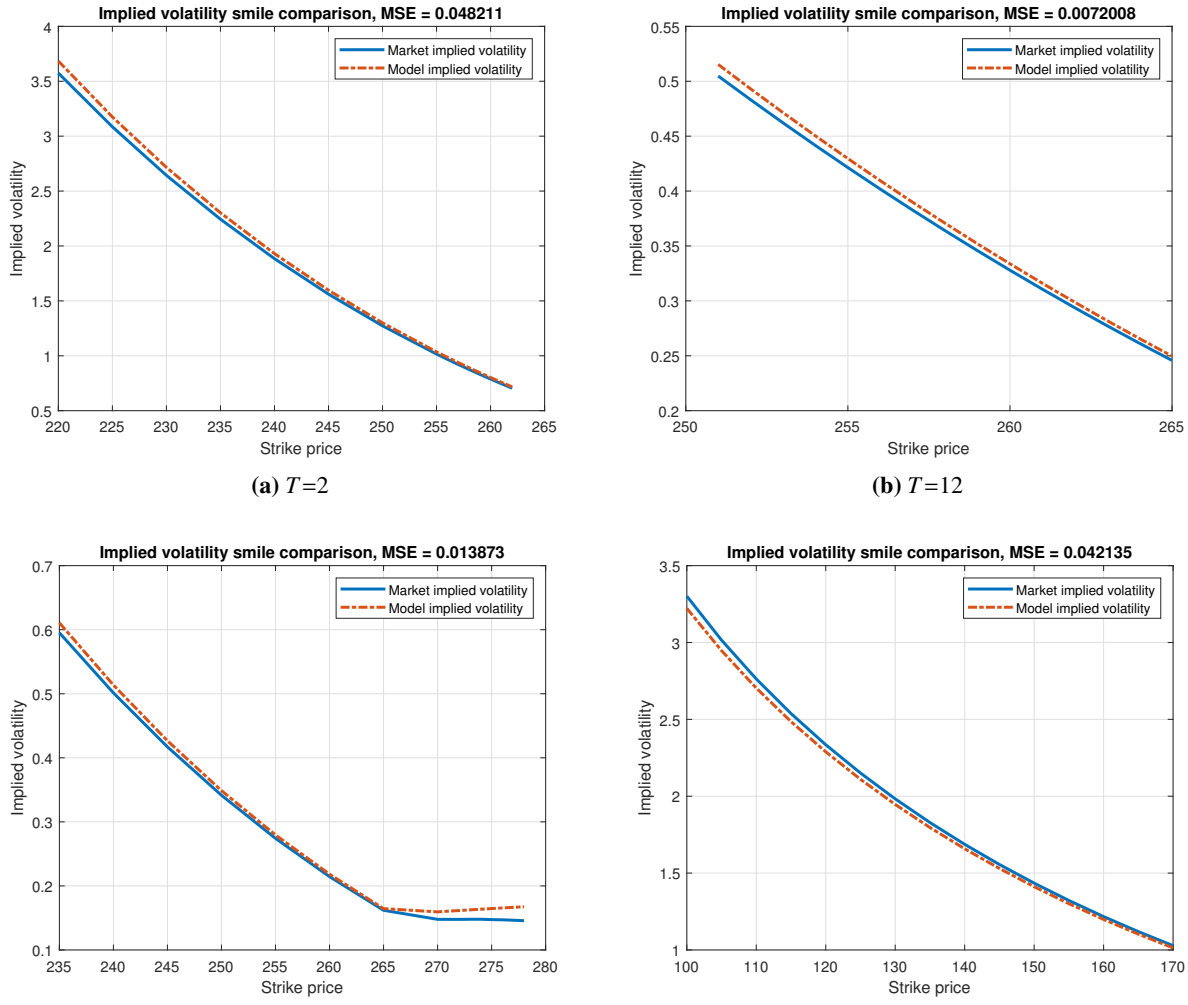

(a) T=2 **(b)** T=12

(c) T=30 **(d)** T=72

Figure 7. Implied volatility smile for T=12 and out-of-sample data.

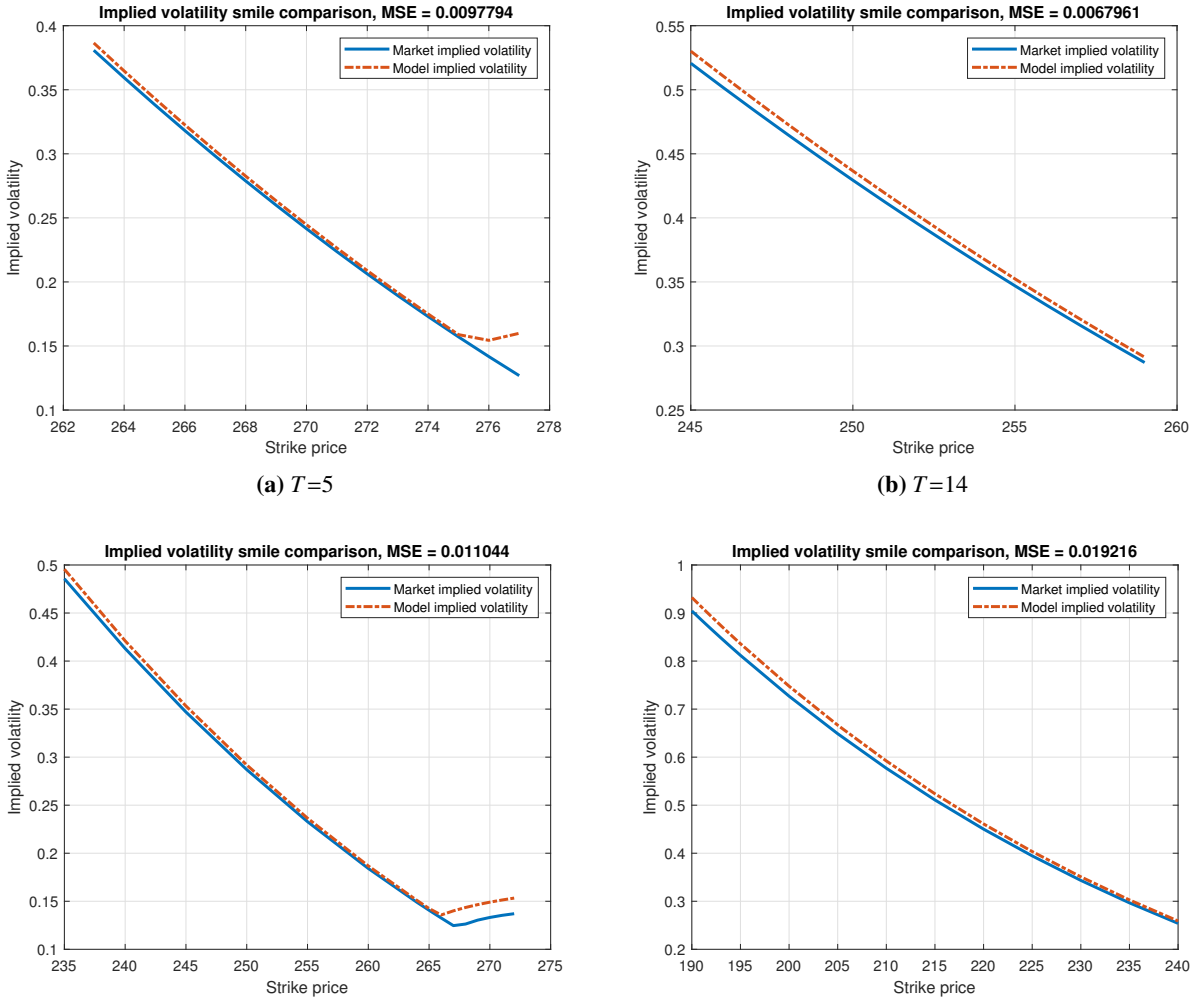

(a) T=5 **(b)** T=14

(c) T=33 **(d)** T=100

Figure 8. Implied volatility smile for out-of-sample data.

6. Conclusions

In financial markets, price jumps and volatility clustering are well-documented phenomena. While the classical rough Bergomi model successfully captures volatility dynamics, it falls short in accounting for sudden price discontinuities. This research addresses this limitation by introducing an extended rough Bergomi model. The proposed model incorporates a jump component into the price process to capture unexpected market events. Additionally, the volatility process is enriched by combining two fractional Brownian motions with identical Hurst parameters, which enhances the model's ability to represent short-term volatility dependencies. To evaluate the model's performance, a risk-neutral measure is established using the Girsanov theorem. This measure ensures that the discounted asset price is a martingale, a fundamental condition for arbitrage-free pricing. Theoretical option prices are derived using the approach outlined by Hull and White [29]. The model's calibration is performed using a pattern search algorithm. The results of the calibration and pricing provide compelling evidence of the proposed model's superior performance. The model successfully reproduces market prices with

high accuracy for both short- and long-term maturities. Analyses showed that the Black-Scholes model, due to its inherent limitation of assuming constant volatility, is unable to accurately reproduce prices across different maturities. This underscores the importance of incorporating volatility dynamics into pricing models. A direct comparison of the proposed model with the classical rough Bergomi model revealed that the addition of extra components, such as the jump process and the hybrid variance curve, significantly enhanced the model's accuracy. Visual evidence from the reproduction of the market's implied volatility surface complements these findings. The proposed model successfully reproduces the observed volatility smile and volatility skew. This capability makes the model a powerful and reliable tool for accurate pricing, risk management, and analyses of market dynamics.

However, this study also highlighted a significant challenge in the calibration process: the algorithm's tendency to get stuck in local optima. This phenomenon indicates that for calibrating complex models, using global optimization algorithms or hybrid approaches is essential. Overall, the results of this research emphasize the importance of using advanced financial models to fully capture market complexities and pave the way for future research in developing and optimizing pricing models. While the results validate the proposed model's credibility and performance, they also shed light on new areas for future research in derivative pricing. These suggestions are based on two main pillars: model development and improvement of calibration methods. One limitation of the current models is the assumption of market homogeneity. For greater realism, heterogeneous processes could be incorporated into the model. For instance, different volatility processes with varying jump rates and parameters could be used for different market segments (e.g., high- and low-liquidity stocks). Additionally, as this study showed, local optimization algorithms like the pattern search were unsuccessful in finding the global optimum. Future research could focus on using global optimization algorithms, such as genetic algorithms or particle swarm optimization, for more precise model calibration.

Author contributions

Zhengfang Long: Formal analysis, Methodology, Writing–original draft; Arezou Karimi: Software, Validation, Writing–original draft, Writing–review & editing; Farshid Mehrdoust: Software, Resources, Writing–original draft. All authors have read and agreed to the published version of the manuscript.

Use of Generative-AI tools declaration

The authors declare they have not used Artificial Intelligence (AI) tools in the creation of this article.

Conflict of interest

The authors declare no conflicts of interest.

References

1. F. Black, M. Scholes, The pricing of options and corporate liabilities, *J. Polit. Econ.*, **81** (1973), 637–654. https://doi.org/10.1086/260062

2. R. C. Merton, Option pricing when underlying stock returns are discontinuous, *J. Financ. Econ.*, **3** (1976), 125–144. https://doi.org/10.1016/0304-405X(76)90022-2

3. D. S. Bates, Jumps and stochastic volatility: exchange rate processes implicit in deutsche mark options, *Rev. Financ. Stud.*, **9** (1996), 69–107. https://doi.org/10.1093/rfs/9.1.69

4. S. L. Heston, A closed-form solution for options with stochastic volatility with applications to bond and currency options, *Rev. Financ. Stud.*, **6** (1993), 327–343. https://doi.org/10.1093/rfs/6.2.327

5. S. G. Kou, A jump-diffusion model for option pricing, *Management Sci.*, **48** (2002), 1086–1101. https://doi.org/10.1287/mnsc.48.8.1086.166

6. T. S. Zaevski, Y. S. Kim, F. J. Fabozzi, Option pricing under stochastic volatility and tempered stable Lévy jumps, *Int. Rev. Financ. Anal.*, **31** (2014), 101–108. https://doi.org/10.1016/j.irfa.2013.10.004

7. Y. X. Tian, H. Y. Zhang, European option pricing under stochastic volatility jump-diffusion models with transaction cost, *Comput. Math. Appl.*, **79** (2020), 2722–2741. https://doi.org/10.1016/j.camwa.2019.12.001

8. Q. Li, L. Wang, Option pricing under jump diffusion model, *Statist. Probab. Lett.*, **211** (2024), 110137. https://doi.org/10.1016/j.spl.2024.110137

9. J. E. Hilliard, J. Hilliard, J. T. D. Ngo, Implied parameter estimation for jump diffusion option pricing models: pricing accuracy and the role of loss and evaluation functions, *J. Commod. Mark.*, **35** (2024), 100408. https://doi.org/10.1016/j.jcomm.2024.100408

10. X. J. He, S. Lin, Analytically pricing foreign exchange options under a three-factor stochastic volatility and interest rate model: a full correlation structure, *Expert Syst. Appl.*, **246** (2024), 123203. https://doi.org/10.1016/j.eswa.2024.123203

11. H. Mesgarani, Y. E. Aghdam, A. Beiranvand, J. F. Gómez-Aguilar, A novel approach to fuzzy based efficiency assessment of a financial system, *Comput. Econom.*, **63** (2024), 1609–1626. https://doi.org/10.1007/s10614-023-10376-5

12. J. G. Wu, J. F. Gomez-Aguilar, R. Taleghani, Portfolio optimization under the uncertain financial model, *Comput. Econom.*, **66** (2025), 571–592. https://doi.org/10.1007/s10614-024-10727-w

13. J. Gatheral, T. Jaisson, M. Rosenbaum, Volatility is rough, 2014, arXiv: 1410.3394.

14. C. Bayer, P. Friz, J. Gatheral, Pricing under rough volatility, *Quant. Finance*, **16** (2016), 887–904. https://doi.org/10.1080/14697688.2015.1099717

15. A. Jacquier, C. Martini, A. Muguruza, On VIX futures in the rough Bergomi model, *Quant. Finance*, **18** (2018), 45–61.

16. O. El Euch, M. Rosenbaum, The characteristic function of rough Heston models, *Math. Finance*, **29** (2019), 3–38. https://doi.org/10.1111/mafi.12173

17. B. Horvath, A. Jacquier, P. Tankov, Volatility options in rough volatility models, *SIAM J. Financ. Math.*, **11** (2020), 437–469. https://doi.org/10.1137/18M1169242

18. E. Alòs, J. A. León, An intuitive introduction to fractional and rough volatilities, *Mathematics*, **9** (2021), 1–22. https://doi.org/10.3390/math9090994

19. J. T. Ma, H. F. Wu, A fast algorithm for simulation of rough volatility models, *Quant. Finance*, **22** (2022), 447–462. https://doi.org/10.1080/14697688.2021.1970213

20. K. Z. Tong, A. Liu, The valuation of barrier options under a threshold rough Heston model, *J. Manag. Sci. Eng.*, **8** (2023), 15–31. https://doi.org/10.1016/j.jmse.2022.07.004

21. Z. G. Shi, P. Lyu, J. T. Ma, High-order methods for the option pricing under multivariate rough volatility models, *Comput. Math. Appl.*, **139** (2023), 173–183. https://doi.org/10.1016/j.camwa.2022.05.039

22. S. Bianchi, D. Angelini, A. Pianese, M. Frezza, Rough volatility via the Lamperti transform, *Commun. Nonlinear Sci. Numer. Simul.*, **127** (2023), 107582. https://doi.org/10.1016/j.cnsns.2023.107582

23. J. L. Dupret, J. Barbarin, D. Hainaut, Impact of rough stochastic volatility models on long-term life insurance pricing, *Eur. Actuar. J.*, **13** (2023), 235–275. https://doi.org/10.1007/s13385-022-00317-1

24. Q. W. Zhu, X. D. Diao, C. F. Wu, Volatility forecast with the regularity modifications, *Finance Res. Lett.*, **58** (2023), 104008. https://doi.org/10.1016/j.frl.2023.104008

25. D. Hainaut, Pricing of spread and exchange options in a rough jump-diffusion market, *J. Comput. Appl. Math.*, **419** (2023), 114752. https://doi.org/10.1016/j.cam.2022.114752

26. A. Karimi, F. Mehrdoust, M. Salahi, Two-factor rough Bergomi model: American call option pricing and calibration by interior point optimization algorithm, *Comput. Econ.*, **66** (2025), 681–714. https://doi.org/10.1007/s10614-024-10725-y

27. A. Karimi, F. Mehrdoust, Modeling logarithmic volatility under the rough fractional Langevin equation: approximation equation and parameter estimation, *Ann. Financ. Econ.*, **20** (2025), 2550005. https://doi.org/10.1142/S2010495225500058

28. P. Gassiat, On the martingale property in the rough Bergomi model, *Electron. Commun. Probab.*, **24** (2019), 1–9. https://doi.org/10.1214/19-ECP239

29. J. Hull, A. White, The pricing of options on assets with stochastic volatilities, *J. Finance*, **42** (1987), 281–300. https://doi.org/10.1111/j.1540-6261.1987.tb02568.x

30. R. Hooke, T. A. Jeeves, "Direct search" solution of numerical and statistical problems, *J. ACM (JACM)*, **8** (1961), 212–229.

31. A. Eberle, *Stochastic analysis*, University of Bonn, 2012.

Appendix A1

The proof of Theorem 2.4 is as follows:

Proof. The existence of solutions to the equation is guaranteed by Theorem 4.4 in [31]. We prove the uniqueness of the solution.

Let us consider two solutions, S_t and $\bar{S}_t$, to Eq (2.9). These solutions correspond to the initial values S_0 and $\bar{S}_0$ respectively. Our goal is to prove that these two solutions are identical, i.e., $S_t = \bar{S}_t$. For any positive integer n, we introduce a stopping time defined as

$$\bar{\tau}_n := \inf\{t \in [0, T] : |r_t| \geq n\},$$

and

$$\hat{\tau}_n := \inf\{t \in [0,T] : |\xi_t| \geq n\}.$$

Set $\tau_n = \bar{\tau}_n \wedge \hat{\tau}_n$. Then,

$$\begin{aligned}
\mathbb{E}\left[\left|S_{t\wedge\tau_n} - \bar{S}_{t\wedge\tau_n}\right|^2\right] &= \mathbb{E}\left[\left|S_0 - \bar{S}_0 + \int_0^{t\wedge\tau_n}\Big(f(u,S_u,\xi_u,r_u) - f(u,\bar{S}_u,\xi_u,r_u)\Big)du\right.\right.\\
&\quad + \int_0^{t\wedge\tau_n}\Big(g(u,S_u,\xi_u,r_u) - g(u,\bar{S}_u,\xi_u,r_u)\Big)dW_u^{\mathbb{Q}}\\
&\quad \left.\left. + \int_{(0,t\wedge\tau_n]\times D}\Big(c_{u^-}(S,y) - c_{u^-}(\bar{S},y)\Big)d\tilde{N}^{\mathbb{Q}}(dudy)\right|^2\right]\\
&\leq \mathbb{E}\left[4\left|S_0 - \bar{S}_0\right|^2 + 4\left|\int_0^{t\wedge\tau_n}\Big(f(u,S_u,\xi_u,r_u) - f(u,\bar{S}_u,\xi_u,r_u)\Big)du\right|^2\right.\\
&\quad + 4\left|\int_0^{t\wedge\tau_n}\Big(g(u,S_u,\xi_u,r_u) - g(u,\bar{S}_u,\xi_u,r_u)\Big)dW_u^{\mathbb{Q}}\right|^2\\
&\quad \left. +4\left|\int_{(0,t\wedge\tau_n]\times D}\Big(c_{u^-}(S,y) - c_{u^-}(\bar{S},y)\Big)d\tilde{N}^{\mathbb{Q}}(dudy)\right|^2\right].
\end{aligned}$$

Applying Ito's isometry, we get

$$\begin{aligned}
\mathbb{E}\left[\left|S_{t\wedge\tau_n} - \bar{S}_{t\wedge\tau_n}\right|^2\right] &\leq 4\mathbb{E}\left[\left|S_0 - \bar{S}_0\right|^2\right] + 4t\mathbb{E}\left[\left|\int_0^{t\wedge\tau_n}\Big(f(u,S_u,\xi_u,r_u) - f(u,\bar{S}_u,\xi_u,r_u)\Big)^2du\right|\right]\\
&\quad + 4\mathbb{E}\left[\left|\int_0^{t\wedge\tau_n}\Big(g(u,S_u,\xi_u,r_u) - g(u,\bar{S}_u,\xi_u,r_u)\Big)^2du\right|\right]\\
&\quad + 4\mathbb{E}\left[\int_0^{t\wedge\tau_n}\int\left|c_{u^-}(S,y) - c_{u^-}(\bar{S},y)\right|^2m(dy)du\right].
\end{aligned}$$

Assumption 2.1 gives

$$\mathbb{E}\left[\left|S_{t\wedge\tau_n} - \bar{S}_{t\wedge\tau_n}\right|^2\right] \leq 4\mathbb{E}\left[\left|S_0 - \bar{S}_0\right|^2\right] + 4\mathcal{K}_n(t+3)\int_0^{t\wedge\tau_n}\mathbb{E}\left[\left|S_u - \bar{S}_u\right|^2\right]du.$$

Define

$$\gamma(t\wedge\tau_n) := \mathbb{E}\left[\left|S_{t\wedge\tau_n} - \bar{S}_{t\wedge\tau_n}\right|^2\right].$$

In this case, $\gamma(t\wedge\tau_n)$ satisfies in the following inequality:

$$\gamma(t\wedge\tau_n) \leq F + G\int_0^{t\wedge\tau_n}\gamma(s)ds,$$

where $F = 4E\left[\left|S_0 - \bar{S}_0\right|^2\right]$ and $G = 4\mathcal{K}_n(t+3)$. Hence, the Gronwall inequality yields that

$$\gamma(t\wedge\tau_n) \leq Fe^{G(t\wedge\tau_n)}.$$

Assuming $S_0 = \bar{S}_0$ when $n \to \infty$, we conclude

$$\mathbb{P}\left[\left|S_t - \bar{S}_t\right| = 0, \forall t \in [0,T]\right] = 1.$$

Therefore, $S(t) = \bar{S}(t)$ for all $0 \leq t \leq T$ almost surely, which proves the uniqueness.

Appendix A2

The pseudo-code for calibration of the proposed model is presented in Algorithm A.1.

Algorithm A.1 Monte Carlo simulation for calibration of the proposed model

Input: Initial parameters θ, number of paths m, number of time steps n, strikes $\{K_1, \ldots, K_u\}$
Output: Model-implied option prices P_k^{Model} for $k = 1, \ldots, u$
for j = 1 to m **do**
    Simulate volatility path $V_{t_0}^j, \ldots, V_{t_n}^j$ using mixed fractional Brownian motion with jumps
    Compute the integrated variance:

$$\bar{V}^j = \sum_{i=0}^{n-1} \frac{V_{t_i}^j + V_{t_{i+1}}^j}{2} \Delta t$$

    for k = 1 to u **do**
        Compute the European call payoff φ_k^j for strike K_k including jump adjustment
    end for
end for
for k = 1 to u **do**
    Compute the Monte Carlo estimate:

$$\mathcal{P}_k^{\text{Model}} = \frac{1}{m} \sum_{j=1}^{m} \varphi_k^j$$

end for